UPPER BOUND ANALYSIS OF BIMETALLIC ROD EXTRUSION PROCESS THROUGH ROTATING CONICAL DIES

HESHMATOLLAH HAGHIGHAT, MOHAMMAD M. MAHDAVI

Mechanical Engineering Department, Razi University, Kermanshah, Iran

e-mail: hhaghighat@razi.ac.ir

In this paper, an upper bound approach is used to analyze the bimetallic rod extrusion process through rotating conical dies. By extending the kinematically admissible velocity field for mono-metal rod extrusion to the bimetallic rod extrusion process, the internal power and the power dissipated on frictional and velocity discontinuity surfaces are evaluated. Then, by equating the total power with the external power produced by axial movement of the punch and the power induced by rotation of the die, the relative extrusion pressure is determined. The extrusion process of bimetallic rods composed of a copper sleeve layer and an aluminium core layer through a conical rotating die is also simulated by using the finite element code ABAQUS. The analytical results are compared with the results given by the finite element method. These comparisons show a good agreement.

Key words: bimetallic rod, extrusion, rotating die, upper bound method, FEM

1. Introduction

Bimetals are components made up of two separate metallic units, each occupying a distinct position in the component. Bimetal components make it possibile to combine properties of dissimilar metals to achieve a structure with low density, good corrosion properties and high strength. The compressive state of stress in extrusion and the possibility of producing metallurgical bonds between the two metals make this process a suitable choice for producing bimetal rods (Berski *et al.*, 2004). In this process, alike other metal forming processes, the estimation and minimization of the extrusion pressure is important.

A number of researches have used the upper bound method and FEM to analyze the bi--metal extrusion process. Avitzur (1983) summarized the factors that affect simultaneous flow of layers in extrusion of a bimetal rod through conical dies. Tokuno and Ikeda (1991) verified the deformation in extrusion of composite bars by experimental and upper bound methods. Sliwa (1997) described the plastic zones in forward extrusion of metal composites by experimental and upper bound methods. Kang *et al.* (2002) designed the die for hot forward and backward extrusion process of Al-Cu clad composite by experimental investigation and FEM simulation. Hwang and Hwang (2002) studied the plastic deformation behavior within a conical die during composite bar extrusion by experimental and upper bound methods.

The making use of rotating dies in metal forming processes was firstly introduced by Greenwood and Thompson (1931). Brovrnan (1987) obtained an analytical solution based on stress analysis for material flow through a rotating conical die excluding the circumferential slipping effect. The so called KOBO type forming proposed by Bochniak and Korbel (1999, 2000, 2003) applied to extrusion of tubes and wires has demonstrated essential advantages with respect to monotonic forming processes. Kim and Park (2003) studied the backward extrusion process with low die rotation to improve the problems of conventional backward extrusion process: the requirement of large forming machine, the difficulty in selecting the die material caused by high surface pressure, high cost of forming machine caused by improvement of noise and vibration,

etc. They used the upper bound technique and FEM simulation. The results showed that the backward extrusion with die rotation is a very useful process, because this process yields homogeneous deformations and lower forming load. Ma *et al.* (2004a,b, 2005) analysed the process of mono-metal rod extrusion through steadily rotating conical dies, theoretically and experimentally. They provided required torque for rotating the die from an external source and also supposed that the angular velocity of the material inside the die changes with power relation to the radius of each position in proportion to apex of virtual conic of the die. They inspected the effect of slippage factor and semi die angle in extrusion pressure and finally determined the optimum die angle. Maciejewski and Mroz (2008) analyzed the mono-metal rod extrusion process through a flat die assisted by cyclic torsion, which was induced by a cyclically rotating die. The evolution of the extrusion force and torsional moment was studied with process parameters such as the ratio of extrusion and rotation rates as well as the amplitude of die rotation.

In this study, the die rotation is proposed to reduce extrusion pressure in the bimetallic rod extrusion process through conical dies. A velocity field for flow of a mono-metal rod during extrusion through a rotating conical die, developed by Ma *et al.* (2004b) is used for the bimetallic rod extrusion process through a conical die in the upper bound model. The FEM simulation on the extrusion of the bimetallic rod composed of a copper sleeve layer and an aluminum core layer is also conducted. The derived upper bound solution allows the correlation of the extrusion pressure with parameters of the process.

2. Upper bound analysis

Based on the upper bound theory, for a rigid-plastic Von-Misses material, the external power required for material deformation is expressed as

$$J^* = \frac{2\sigma_o}{\sqrt{3}} \int_V \sqrt{\frac{1}{2}\dot{\varepsilon}_{ij}\dot{\varepsilon}_{ij}} \, dV + \int_{S_v} k|\Delta V| \, dS + m \int_{S_f} k|\Delta V| \, dS - \int_{S_t} T_i v_i \, dS \qquad (2.1)$$

where σ_o is the mean flow stress of the material, k – material yield strength in shear, $\dot{\varepsilon}_{ij}$ – strain rate tensor, m – constant friction factor, V – volume of plastic deformation zone, S_v and S_f – area of velocity discontinuity and frictional surfaces, respectively, S_t – area where the tractions may occur, ΔV – amount of velocity discontinuity on the frictional and discontinuity surfaces and v_i and T_i are the velocity and tractions applied on S_t, respectively.

The rotational bimetallic rod extrusion process consists of an axial movement of the punch and the rotational movement of the die. Figure 1 shows a schematic diagram of the bimetallic rod extrusion through a rotating conical die shape. An initially bimetallic rod, made up of a rod and an annular tube of two different ductile materials with the mean flow stresses σ_c and σ_s, respectively, is considered. The initial outer and inner radius of the combined rod is R_{1i} and R_{2i}, respectively. The outer radius of the extruded bimetallic rod is R_{1f} and the interface radius of the final extruded rod is R_{2f}.

To analyze the process, the material under deformation is divided into eight zones, as shown in Fig. 1. A spherical coordinate system (r, θ, φ) with the origin O is used to describe the position of the four surfaces of velocity discontinuity S_1-S_4 as well as the velocity in deformation zones I and II. In zones VII and VIII, the incoming materials are assumed to flow horizontally as a rigid body with velocity v_i. In zones V and VI, the extruded bimetallic rod is assumed to flow horizontally as a rigid body with velocity v_f. Zones I to IV are the deformation regions, where the velocity is complex. Zone I is surrounded by surfaces S_1, S_2, the die surface and the interface surface. Zone II is surrounded by surfaces S_3, S_4 and the interface surface.

The material inside the container along the total length L is divided into two segments. Within the length l, the bimetallic rod is twisted plastically inside the container and the regions
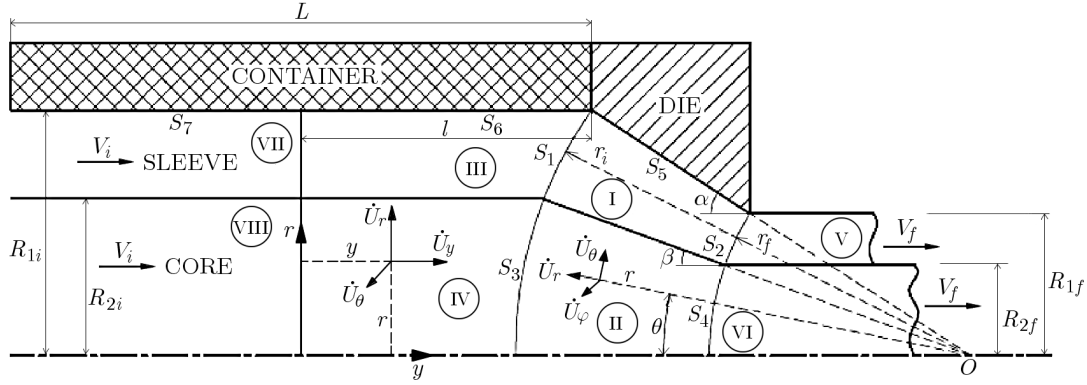
Fig. 1. Schematic diagram of bimetallic rod extrusion process through a rotating conical die, geometric parameters and its deformation zones

enclosed are denoted as zones III and IV. A cylindrical coordinate system (r, θ, y) is used to describe the velocity field in deformation zones III and IV where the axial coordinate y is parallel to the extruding direction. The bimetallic rod in the remaining length $(L - l)$ is designated by zones VII and VIII. In these zones, the incoming material is assumed to flow horizontally as a rigid body with velocity v_o.

The surfaces S_1 and S_3 are located at distance r_i from the origin, and the surfaces S_2 and S_4 are located at distance r_f from the origin. The mathematical equations for radial positions of the four velocity discontinuity surfaces S_1, S_3 and S_2, S_4 are given by

$$r_i = \frac{R_{1i}}{\sin \alpha} \qquad r_f = \frac{R_{1f}}{\sin \alpha} \tag{2.2}$$

where α is the semi die angle.

In addition to these surfaces, there are three frictional surfaces between the die wall and sleeve S_5, between the twisted surface of the sleeve material inside the container and container surface S_6, and between the container and sleeve S_7.

The interface surface between the inner and the outer materials is defined by the angle β, shown in Fig. 1, defined as

$$\sin \beta = \frac{R_{1i}}{R_{2i}} \sin \alpha \tag{2.3}$$

The first step in modeling and analysing a metal forming process by the use of the upper bound approach is to select a suitable velocity field for the material which is deformed plastically.

2.1. Velocity fields and power terms for deformation zones I and II

For deformation zones I and II, the same velocity field proposed by Ma *et al.* (2004b) for mono-metal rod extrusion process through a rotating conical die is extended here for flow of the bimetallic rod extrusion through rotating conical dies. So the velocity field is described by following spherical components

$$\dot{U}_r = -v_f \left(\frac{r_f}{r}\right)^2 \cos \theta \qquad \dot{U}_\theta = 0 \qquad \dot{U}_\varphi = \eta_1 \dot{\omega}_d \sin \theta \frac{r_f^3}{r^2} \tag{2.4}$$

where $\dot{\omega}_d$ is the angular velocity of the die and η is the slippage parameter (angular velocity ratio of the bimetallic rod at the exit of the conical die to the rotating die).

For the present work, the bonding condition between the core and the sleeve is assumed to be sticky and there is no slippage between the core and sleeve materials.

The strain rates in spherical coordinates are defined as

$$\dot{\varepsilon}_{rr} = \frac{\partial \dot{U}_r}{\partial r} = 2v_f r_f^2 \frac{\cos\theta}{r^3} \qquad\qquad \dot{\varepsilon}_{\theta\theta} = \frac{1}{r}\frac{\partial \dot{U}_\theta}{\partial\theta} + \frac{\dot{U}_r}{r} = -v_f r_f^2 \frac{\cos\theta}{r^3}$$

$$\dot{\varepsilon}_{\varphi\varphi} = \frac{1}{r\sin\theta}\frac{\partial \dot{U}_\varphi}{\partial\varphi} + \frac{\dot{U}_r}{r} + \frac{\dot{U}_\theta}{r}\cot\theta = -v_f r_f^2 \frac{\cos\theta}{r^3}$$

$$\dot{\varepsilon}_{r\theta} = \frac{1}{2}\Big(\frac{\partial \dot{U}_\theta}{\partial r} - \frac{\dot{U}_\theta}{r} + \frac{1}{r}\frac{\partial \dot{U}_r}{\partial\theta}\Big) = \frac{1}{2}v_f r_f^2 \frac{\sin\theta}{r^3} \tag{2.5}$$

$$\dot{\varepsilon}_{\theta\varphi} = \frac{1}{2}\Big(\frac{1}{r\sin\theta}\frac{\partial \dot{U}_\theta}{\partial\varphi} + \frac{1}{r}\frac{\partial \dot{U}_\varphi}{\partial\theta} - \frac{\cot\theta}{r}\dot{U}_\varphi\Big) = 0$$

$$\dot{\varepsilon}_{\varphi r} = \frac{1}{2}\Big(\frac{\partial \dot{U}_\varphi}{\partial r} - \frac{\dot{U}_\varphi}{r} + \frac{1}{r\sin\theta}\frac{\partial \dot{U}_r}{\partial\varphi}\Big) = -\frac{1}{2}\eta_1\dot{\omega}_d r_f^3 \frac{3\sin\theta}{r^3}$$

where $\dot{\varepsilon}_{ii}$ (with $i = j$) is the shear strain rate component.

With the strain rate tensor and the velocity field, the standard upper bound method can be implemented. This method involves calculating the internal power of deformation over the deformation zones volume, the shear power losses over two surfaces of velocity discontinuity, and the frictional power losses between the workpiece and tool.

The internal power dissipated in the deformation zone is given by

$$\dot{W}_i = \frac{2\sigma_o}{\sqrt{3}}\int\limits_V \sqrt{\frac{1}{2}\dot{\varepsilon}_{ij}\dot{\varepsilon}_{ij}}\; dV \tag{2.6}$$

For deformation zone I that is surrounded by two velocity discontinuity surfaces S_1, S_2, the interface surface and the die surface, substituting the strain rate tensor from Eqs. (2.5) into Eq. (2.6) and noting that $dV = 2\pi r^2 \sin\theta\, dr d\theta$, the internal power of deformation becomes

$$\dot{W}_{i1} = 2\pi\frac{2\sigma_s}{\sqrt{3}}\int\limits_{r_f}^{r_o}\int\limits_\beta^\alpha \sqrt{\frac{1}{2}\dot{\varepsilon}_{rr}^2 + \frac{1}{2}\dot{\varepsilon}_{\theta\theta}^2 + \frac{1}{2}\dot{\varepsilon}_{\varphi\varphi}^2 + \dot{\varepsilon}_{r\theta}^2 + \dot{\varepsilon}_{\varphi r}^2}\; r^2\sin\theta\, d\theta\, dr \tag{2.7}$$

where σ_s is the mean flow stress of the sleeve, which is determined by

$$\sigma_s = \frac{1}{\varepsilon}\int\limits_0^\varepsilon \sigma\, d\varepsilon \qquad\qquad \varepsilon = \ln\frac{R_{1i}^2 - R_{2i}^2}{R_{1f}^2 - R_{2f}^2} \tag{2.8}$$

The internal power of deformation in zone II becomes

$$\dot{W}_{i2} = 2\pi\frac{2\sigma_c}{\sqrt{3}}\int\limits_{r_f}^{r_o}\int\limits_0^\beta \sqrt{\frac{1}{2}\dot{\varepsilon}_{rr}^2 + \frac{1}{2}\dot{\varepsilon}_{\theta\theta}^2 + \frac{1}{2}\dot{\varepsilon}_{\varphi\varphi}^2 + \dot{\varepsilon}_{r\theta}^2 + \dot{\varepsilon}_{\theta\varphi}^2 + \dot{\varepsilon}_{\varphi r}^2}\; r^2\sin\theta\, d\theta\, dr \tag{2.9}$$

where σ_c is the mean flow stress of the core, given by

$$\sigma_c = \frac{1}{\varepsilon}\int\limits_0^\varepsilon \sigma\, d\varepsilon \qquad\qquad \varepsilon = \ln\frac{R_{2i}^2}{R_{2f}^2} \tag{2.10}$$

The general equation for the power losses along the shear surface of velocity discontinuity in the upper bound model is

$$\dot{W}_S = \frac{\sigma_o}{\sqrt{3}}\int\limits_S |\Delta V|\, dS \tag{2.11}$$

where for the velocity discontinuity surfaces S_1 and S_3

$$\Delta V_1 = v_o \sin\theta \qquad\qquad dS_1 = 2\pi r_o^2 \sin\theta \, d\theta \qquad\qquad (2.12)$$

For the velocity discontinuity surfaces S_2 and S_4

$$\Delta V_2 = v_f \sin\theta \qquad\qquad dS_2 = 2\pi r_f^2 \sin\theta \, d\theta \qquad\qquad (2.13)$$

Inserting Eqs. (2.12) and (2.13) into Eq. (2.11), the power dissipated on the velocity discontinuity surfaces S_1, S_2, S_3 and S_4 are determined as

$$
\begin{aligned}
\dot{W}_{S_1} &= \pi \frac{\sigma_s}{\sqrt{3}} v_o r_o^2 \Big(\alpha - \beta - \frac{\sin 2\alpha - \sin 2\beta}{2} \Big) &\qquad \dot{W}_{S_3} &= \pi \frac{\sigma_c}{\sqrt{3}} v_o r_o^2 \Big(\beta - \frac{\sin 2\beta}{2} \Big) \\
\dot{W}_{S_2} &= \pi \frac{\sigma_s}{\sqrt{3}} v_f r_f^2 \Big(\alpha - \beta - \frac{\sin 2\alpha - \sin 2\beta}{2} \Big) &\qquad \dot{W}_{S_4} &= \pi \frac{\sigma_c}{\sqrt{3}} v_f r_f^2 \Big(\beta - \frac{\sin 2\beta}{2} \Big)
\end{aligned}
\qquad (2.14)
$$

The general equation for the frictional power losses along the surface with a constant friction factor m is

$$\dot{W}_f = m \frac{\sigma_o}{\sqrt{3}} \int\limits_{S_f} |\Delta V| \, dS \qquad\qquad (2.15)$$

For the conical surface of the die, the frictional surface S_5, the magnitude of the velocity difference and the differential surface are

$$\Delta V_3 = \sqrt{\Delta V_r^2 + \Delta V_\varphi^2} \qquad\qquad dS_3 = 2\pi r \sin\alpha \, dr \qquad\qquad (2.16)$$

where

$$\Delta V_r = \dot{U}_r \Big|_{\theta=\alpha} = v_f r_f^2 \frac{\cos\alpha}{r^2} \qquad\qquad \Delta V_\varphi = r \sin\alpha \dot{\omega}_d - \dot{U}_\varphi \Big|_{\theta=\alpha} = r \sin\alpha \dot{\omega}_d \Big(1 - \frac{\eta r_f^3}{r^3} \Big) \quad (2.17)$$

Inserting Eqs. (2.17) into Eq. (2.16) and then placing into Eq. (2.15), gives the frictional power losses along the conical surface of the die as

$$\dot{W}_{f3} = 2\pi \frac{m_d \sigma_c}{\sqrt{3}} \int\limits_{r_f}^{r_o} \sqrt{ \Big(v_f r_f^2 \frac{\cos\alpha}{r^2} \Big)^2 + \Big[r \sin\alpha \dot{\omega}_d \Big(1 - \eta_1 \frac{r_f^3}{r^3} \Big) \Big]^2 } \; r \sin\alpha \, dr \qquad (2.18)$$

where m_d is the constant friction factor between the sleeve material and the die.

2.2. Velocity fields and power terms for deformation zone III

For deformation zone III and IV, using the cylindrical coordinate system (r, θ, y) in Fig. 1, the same components of the velocity field were employed by Ma *et al.* (2004b) in the deformation zone III to analyze the mono-metal rod extrusion process through rotating conical dies

$$\dot{U}_y = v_o \qquad\qquad \dot{U}_r = 0 \qquad\qquad \dot{U}_\theta = \eta_2 \dot{\omega}_d r \frac{y}{l} \qquad \text{with} \quad \eta_2 = \eta_1 \Big(\frac{r_f}{r_o} \Big)^3 \qquad (2.19)$$

where η_2 is the slippage parameter (angular velocity ratio of the bimetallic rod at the entrance of the conical die to the rotating die).

The strain rates in cylindrical coordinates are defined as

$$
\begin{aligned}
&\dot{\varepsilon}_{rr} = \frac{\partial \dot{U}_r}{\partial r} = 0 && \dot{\varepsilon}_{\theta\theta} = \frac{1}{r}\frac{\partial \dot{U}_\theta}{\partial \theta} + \frac{\dot{U}_r}{r} = 0 \\[2mm]
&\dot{\varepsilon}_{zz} = \frac{\partial \dot{U}_y}{\partial y} = 0 && \dot{\varepsilon}_{r\theta} = \frac{1}{2}\Big(\frac{\partial \dot{U}_\theta}{\partial r} + \frac{1}{r}\frac{\partial \dot{U}_r}{\partial \theta} - \frac{\dot{U}_\theta}{r}\Big) = 0 \\[2mm]
&\dot{\varepsilon}_{\theta y} = \frac{1}{2}\Big(\frac{\partial \dot{U}_\theta}{\partial y} + \frac{1}{r}\frac{\partial \dot{U}_y}{\partial \theta}\Big) = 0 && \dot{\varepsilon}_{yr} = \frac{1}{2}\Big(\frac{\partial \dot{U}_r}{\partial y} + \frac{\partial \dot{U}_y}{\partial r}\Big) = 0 \\[2mm]
&\dot{\varepsilon}_{y\theta} = \frac{1}{2}\Big(\frac{\partial \dot{U}_\theta}{\partial y} + \frac{1}{r}\frac{\partial \dot{U}_y}{\partial \theta}\Big) = \frac{1}{2}\eta_2\dot{\omega}_d\frac{r}{l} &&
\end{aligned}
\tag{2.20}
$$

Placing Eqs. (2.20) into Eq. (2.6) and noting that $dV = 2\pi r\,dr\,dy$, the internal power of deformation in zone III is determined as

$$
\dot{W}_{i3} = \frac{2\sigma_s}{\sqrt{3}}\int\limits_{R_{1i}}^{R_{2i}}\int\limits_0^l \frac{1}{2}\eta_2\dot{\omega}_d\frac{r}{l}2\pi r\,dr\,dy = \frac{2\pi}{3\sqrt{3}}\sigma_s\eta_2\dot{\omega}_d(R_{1i}^3 - R_{2i}^3)
\tag{2.21}
$$

The internal power of deformation in zone IV is determined as

$$
\dot{W}_{i4} = \frac{2\sigma_c}{\sqrt{3}}\int\limits_0^{R_{2i}}\int\limits_0^l \frac{1}{2}\eta_2\dot{\omega}_d\frac{r}{l}2\pi r\,dr\,dy = \frac{2\pi}{3\sqrt{3}}\sigma_c\eta_2\dot{\omega}_d R_{2i}^3
\tag{2.22}
$$

The power dissipated on the frictional surfaces S_6 and S_7 are also can be obtained by Eq. (2.15). The velocity discontinuity on the surface S_6 and its area become

$$
\Delta V_6 = \sqrt{\Delta V_y^2 + \Delta V_\theta^2} = \sqrt{v_o^2 + \Big(\beta_2\dot{\omega}_d R_{1i}\frac{y}{l}\Big)^2} \qquad dS_7 = 2\pi R_{1i}\,dy
\tag{2.23}
$$

The frictional power losses along the surface S_6 can be given by

$$
\dot{W}_{f6} = \frac{m_c\sigma_s}{\sqrt{3}}\int\limits_0^l \sqrt{v_o^2 + \Big(\eta_2\dot{\omega}_d R_{1i}\frac{y}{l}\Big)^2}\,2\pi R_{1i}\,dy = 2\pi\frac{m_c\sigma_s}{\sqrt{3}}R_{1i}^2\eta_2\dot{\omega}_d A
\tag{2.24}
$$

where

$$
A = \frac{1}{2}\sqrt{\Big(\frac{v_o}{\beta_2\dot{\omega}_d R_{1i}}\Big)^2 + 1} + \frac{l}{2}\Big(\frac{v_o}{\beta_2\dot{\omega}_d R_{1i}}\Big)^2 \ln\frac{\beta_2\dot{\omega}_d R_{1i} + \sqrt{v_o^2 + (\beta_2\dot{\omega}_d R_{1i})^2}}{v_o}
\tag{2.25}
$$

where m_c is the constant friction factor between the sleeve material and the container.

Finally, for the frictional surface S_7

$$
\dot{W}_{f7} = \frac{m_c\sigma_{ys}}{\sqrt{3}}\int\limits_0^{L-l} 2\pi R_{1i}v_o\,dy = 2\pi\frac{m\sigma_{ys}}{\sqrt{3}}R_{1i}v_o(L-l)
\tag{2.26}
$$

where σ_{ys} is the mean flow stress of the sleeve prior to any deformation and L is length of the rod in the container.

2.3. Total power

Based on the upper bound model, the total power needed for the extrusion process can be obtained by summing the internal power and the power dissipated on all frictional and velocity discontinuity surfaces as

$$J^* = \dot{W}_{i1} + \dot{W}_{i2} + \dot{W}_{i3} + \dot{W}_{i4} + \dot{W}_{S1} + \dot{W}_{S2} + \dot{W}_{S3} + \dot{W}_{S4} + \dot{W}_{f5} + \dot{W}_{f6} + \dot{W}_{f7} \qquad (2.27)$$

Therefore, the total upper bound solution for the relative extrusion pressure P_{ave}/σ_o is given by

$$\frac{P_{ave}}{\sigma_s} = \frac{J^* + M_d \dot{\omega}_d}{\pi v_o R_{1i}^2 \sigma_s} \qquad (2.28)$$

All integrals that are presented in the power terms are evaluated by numerical integration. For given extrusion conditions, the total power in the equation above is function of the slippage parameter η_1 and twisting length of the material inside the container l.

As the balance among twisting moments must be maintained, the moment applied by the rotary die is balanced with summing up the moment caused by the circumferential friction in the container. In addition to the power applied by the punch, a twist moment M_d is supplied by the rotating die, and this moment can be calculated as

$$M_d = 2\pi m_d \frac{\sigma_s}{\sqrt{3}} \int_{r_f}^{r_o} \cos\gamma_3 (r\sin\alpha)^2 \, dr \qquad \cos\gamma_3 = \frac{\Delta V_{\varphi 3}}{\Delta V_3} \qquad (2.29)$$

The twist moment within the container is given as

$$M_7' = 2\pi m_c \frac{\sigma_{ys}}{\sqrt{3}} \int_0^l \cos\gamma_7 R_o^2 \, dy \qquad \cos\gamma_7 = \frac{\Delta V_{\theta 7}}{\Delta V_7} \qquad (2.30)$$

The balance of the couples gives

$$M_d = M_7' \qquad (2.31)$$

The twisting length l can be determined by satisfying Eq. (2.32) with a given η_1

$$l = \frac{m_d \sigma_s \int_{r_f}^{r_o} \cos\gamma_3 (r\sin\alpha)^2 \, dr}{m_c \sigma_{ys} R_{1i}^2 \left[-\frac{v_o}{\eta_2 \dot{\omega}_d R_{2i}} + \sqrt{\left(\frac{v_o}{\eta_2 \dot{\omega}_d R_{2i}}\right)^2 + 1} \right]} \qquad (2.32)$$

3. Results and discussion

To make a comparison with the developed model, a bi-metal rod composed of aluminium as the core layer and copper as the sleeve layer, was used. The configuration of the sleeve and core layers is shown in Fig. 2. The flow stresses for copper and aluminium in room temperature were obtained as (Hwang and Hwang, 2002)

$$\sigma_{Al} = 189.2\varepsilon^{0.239} \text{ MPa} \qquad \sigma_{cu} = 335.2\varepsilon^{0.113} \text{ MPa} \qquad (3.1)$$

The extrusion process is simulated by using the finite element code ABAQUS. A three-dimensional model is used for FEM analyses. The billet model is meshed with C3D8R elements.
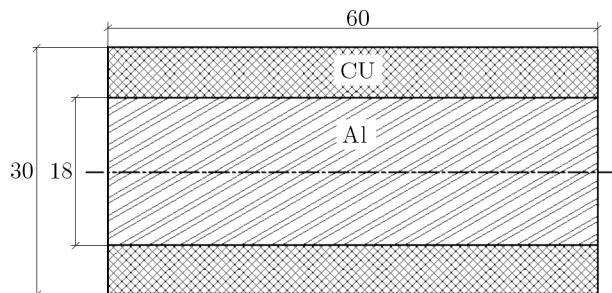
Fig. 2. Configuration of the bimetallic rod before extrusion (dimensions are in mm)

The punch and die are assumed as rigid models. Since the analytical rigid option is used for the rigid bodies, they are not meshed.

The punch model is loaded by specifying displacement in the axial direction, and the die model is able to rotate along the die axis and it is fixed in other directions by applying displacement constraints on its nodes. Figure 3a illustrates the mesh used to analyze the deformation in extrusion of the bimetallic rod with the configuration shown in Fig. 2 and $\alpha = 20°$, $v_o = 1\,\text{mm/s}$, $m_d = 0.2$, $m_c = 0.2$. The deformed models of the sleeve and core are shown in Fig. 3b.
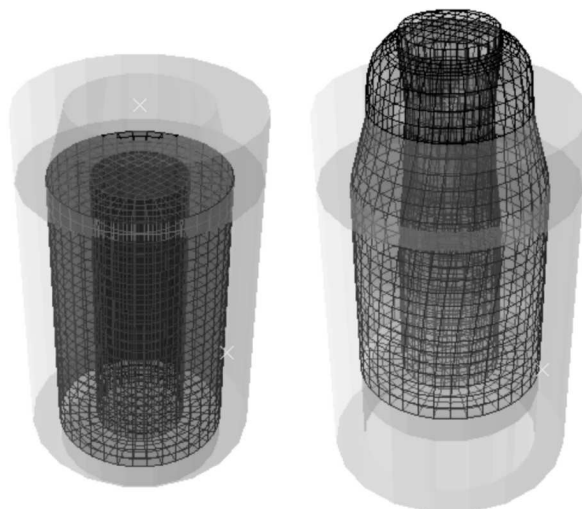
Fig. 3. (a) The finite element mesh and (b) the deformed mesh, in extrusion process of a bimetallic rod through a rotating die

In Fig. 4, the extrusion pressure variation obtained from the upper bound solution is compared with the FEM. The results show a good agreement between the upper bound data and the FEM results. As shown in Fig. 4, the analytically predicted pressure is higher than the FEM result, which is due to the nature of the upper bound theory.

This figure also shows that with the increasing of the angular velocity of the die the relative extrusion pressure is decreased, but this reduction saturates at a high die angular velocity. It can be seen that the relative extrusion pressure is decreased by about 6% by the die rotation.

In Fig. 5, the relative extrusion pressure for different semi-die angles obtained from the upper bound solution is compared with the FEM simulation results. The results show a good agreement between the upper bound data and the FEM results. It is observed that there is an optimal die angle which minimizes the extrusion force.

The effect of angular velocity on the relative extrusion pressure for different values of die friction factors is shown in Fig. 6. It is observed that the extrusion pressure is decreased by growth of the die angular velocity and drop of the die friction factor, but this reduction saturates at a high die angular velocity.
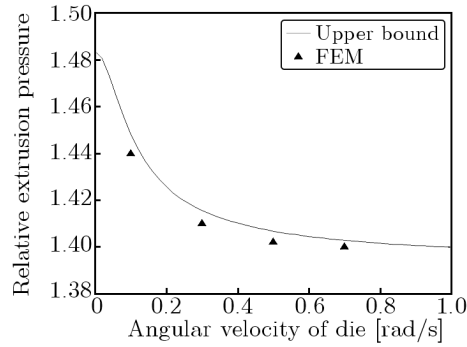
Fig. 4. Comparison of analytical relative extrusion pressure with FEM data for different angular velocities of the die for $\alpha = 20°$, $v_o = 1\,\text{mm/s}$, $R_{1o} = 15\,\text{mm}$, $R_{1f} = 13\,\text{mm}$, $R_{2o} = 9\,\text{mm}$, $m_d = 0.2$, $m_c = 0.2$
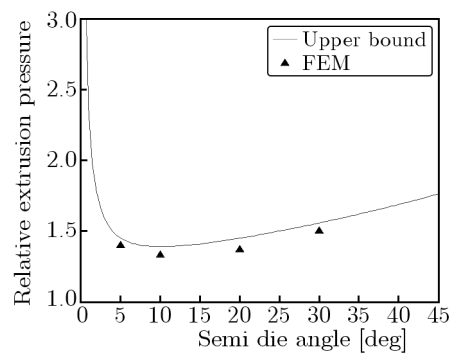
Fig. 5. Comparison of analytical relative extrusion pressure with FEM data for different semi-die angles for $v_o = 1\,\text{mm/s}$, $R_{1o} = 15\,\text{mm}$, $R_{1f} = 13\,\text{mm}$, $R_{2o} = 9\,\text{mm}$, $\omega = 0.1\,\text{rad/s}$, $m_d = 0.2$, $m_c = 0.2$
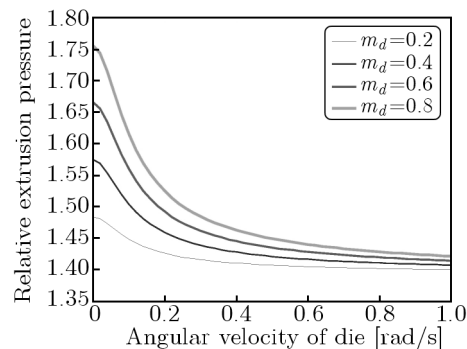
Fig. 6. Effect of angular velocity of the die on the relative extrusion pressure for different friction factors of the die for $\alpha = 20°$, $v_o = 1\,\text{mm/s}$, $R_{1o} = 15\,\text{mm}$, $R_{1f} = 13\,\text{mm}$, $R_{2o} = 9\,\text{mm}$, $m_c = 0.2$

The effect of the die angle on the relative extrusion pressure for different values of die friction factors is shown in Fig. 7. As it is expected, for a given value of die friction factor, there is an optimal die angle which minimizes the extrusion pressure, and the optimum die angle increases when the friction factor increases. This figure also shows that an increase in the friction factor of the die tends to increase the extrusion pressure.

The effect of angular velocity on the relative extrusion pressure for different values of the tube entrance speed is shown in Fig. 8. It is observed that the extrusion pressure is decreased by a drop in the die angular velocity and a drop in the entrance speed, but this reduction is low at high entrance speeds.
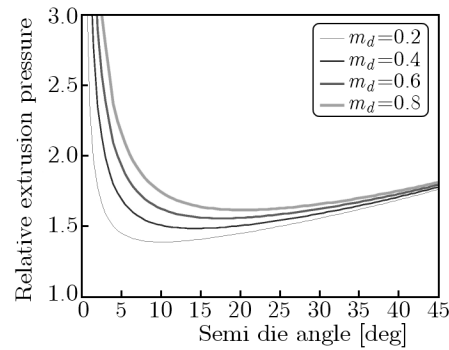
Fig. 7. Effect of semi-die angle on the relative extrusion pressure for different friction factors of the die for $v_o = 1\,\mathrm{mm/s}$, $R_{1o} = 15\,\mathrm{mm}$, $R_{1f} = 13\,\mathrm{mm}$, $R_{2o} = 9\,\mathrm{mm}$, $\omega = 0.1\,\mathrm{rad/s}$, $m_c = 0.2$
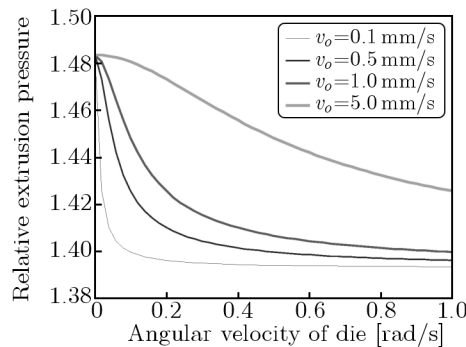
Fig. 8. Effect of angular velocity of the die on reduction of the extrusion pressure for different extruding speeds for $\alpha = 20°$, $R_{1o} = 15\,\mathrm{mm}$, $R_{1f} = 13\,\mathrm{mm}$, $R_{2o} = 9\,\mathrm{mm}$, $m_d = 0.2$, $m_c = 0.2$

4. Conclusions

In this study, an upper bound model for analysis of the bimetallic rod extrusion process through rotating conical dies was developed. Derivations for three main components of the consumed power during the process including deformation, discontinuity, friction power and the relation for calculating the relative extrusion pressure were presented. The results showed a good agreement between the analytical solution and FEM simulation. The developed upper bound solution can be very beneficial in studying the influence of multiple variables on the bimetallic rod extrusion process through rotating conical dies and for a given process parameters. It can be used for finding the optimum die angle which minimizes the extrusion pressure.

References

1. AVITZUR B., 1983, *Handbook of Metal-Forming Processes*, Wiley, New York

2. BERSKI S., DYJA H., BANASZEK G., JANIK M., 2004, Theoretical analysis of bimetal bar extrusion process in double reduction dies, *Journal of Materials Processing Technology*, **154**, 153-183

3. BOCHNIAK W., KORBEL A., 1999, Extrusion of CuZn39Pb2 alloy by the KOBO method, *Engineering Transactions*, **47**, 351-367

4. BOCHNIAK W., KORBEL A., 2000, Plastic flow of aluminum extruded, under complex conditions, *Materials Science and Technology*, **16**, 664-674

5. BOCHNIAK W., KORBEL A., 2003, KOBO-type forming: forging of metals under complex conditions of the process, *Journal of Materials Processing Technology*, **134**, 120-134

6. BROVRNAN M.J., 1987, Steady forming processes of plastic materials with their rotation, *International Journal of Mechanical Sciences*, **29**, 483-489

7. GREENWOOD H., THOMPSON F.C., 1931, Wires drawn through rotating dies, *Nature*, **128**, 152

8. HWANG Y.M., HWANG T.F., 2002, An investigation into the plastic deformation behavior within a conical die during composite bar extrusion, *Journal of Materials Processing Technology*, **121**, 226-233

9. KANG C.G., JUNG Y.J., KWON H.C., 2002, Finite element simulation of die design for hot extrusion process of Al/Cu clad composite and its experimental investigation, *Journal of Materials Processing Technology*, **124**, 49-56

10. KIM Y.H., PARK J.H., 2003, Upper bound analysis of torsional backward extrusion process, *Journal of Materials Processing Technology*, **143/144**, 735-740

11. MA X., BARNETT M.R., KIM Y.H., 2004a, Forward extrusion through steadily rotating conical dies. Part I: experiments. *International Journal of Mechanical Sciences*, **46**, 449-464

12. MA X., BARNETT M.R., KIM Y.H., 2004b, Forward extrusion through steadily rotating conical dies. Part II: theoretical analysis, *International Journal of Mechanical Sciences*, **46**, 465-489

13. MA X., BARNETT M., 2005, An upper bound analysis of forward extrusion through rotating dies, *Proceedings of the 8th ESAFORM Conference on Material Forming*, Bucharest, Romania, 565-568

14. MACIEJEWSKI J., MROZ Z., 2008, An upper-bound analysis of axisymmetric extrusion assisted by cyclic torsion, *Journal of Materials Processing Technology*, **206**, 333-344

15. SLIWA R., 1997, Plastic zones in the extrusion of metal composites, *Journal of Materials Processing Technology*, **67**, 29-35

16. TOKUNO H., IKEDA K., 1991, Analysis of deformation in extrusion of composite bars, *Journal of Materials Processing Technology*, **26**, 323-335